

# Study on Molecular Chain Heterogeneity of Linear Low-Density Polyethylene by Cross-Fractionation of Temperature Rising Elution Fractionation and Successive Self-Nucleation/Annealing Thermal Fractionation

Jie Kong, Xiaodong Fan, Yunchuan Xie, Wenqiang Qiao

Department of Applied Chemistry, School of Science, Northwestern Polytechnical University, Xi'an 710072, China

Received 19 November 2003; accepted 15 May 2004

DOI 10.1002/app.21084

Published online in Wiley InterScience (www.interscience.wiley.com).

**ABSTRACT:** The molecular chain heterogeneity of commercial linear low-density polyethylene (LLDPE) was investigated by cross-fractionation of temperature rising elution fractionation (TREF) and successive self-nucleation/annealing (SSA) thermal fractionation by use of DSC. The results indicate that the linear relationships between crystallinity or melting temperature and the elution temperature are confirmed by TREF fractions. Intermolecular heterogeneity exists in the original LLDPE, whereas there is less intermolecular heterogeneity in the TREF fractions. After SSA thermal fractionation, the multiple endothermic peaks for both LLDPE and their TREF fractions are mainly attributed to the heterogeneities of ethylene sequence length (ESL) and lamel-

lar thickness. The statistical terms, including weighted mean  $\bar{L}_w$ , arithmetic mean  $\bar{L}_n$ , and broad index  $\bar{L}_w/\bar{L}_n$ , were introduced to evaluate the heterogeneities of ESL and lamellar thickness of polyethylene. The difference of broadness index indicates that TREF fractions of LLDPE have less inter- and intramolecular heterogeneities of both ESL and lamellar thickness than those of the original LLDPE. © 2004 Wiley Periodicals, Inc. *J Appl Polym Sci* 94: 1710–1718, 2004

**Key words:** fractionation of polymers; lamellar; ethylene sequence length (ESL); crystallization; linear low-density polyethylene (LLDPE)

## INTRODUCTION

Linear low-density polyethylene (LLDPE), produced by the copolymerization of ethylene and an  $\alpha$ -olefin such as 1-butene, 1-hexene, and 1-octene over either Ziegler–Natta or metallocene catalysts, is characterized by heterogeneity in both molecular mass and short-chain branching (SCB) content and distribution. It consists of two kinds of heterogeneity: intra- and intermolecular. The former concept implies that within one molecular chain, SCB distribution is not uniform along the chain backbone, whereas all the molecules possess the same SCB distribution. The latter concept implies that among the molecules, the SCB distribution is not uniform, that is, the SCB content is higher in some molecules than in others. All these heterogeneities have effects on crystallizability, thermal and mechanical properties, and processing behavior of LLDPE. In particular, the amount and distribution of SCB are dominant factors for determining the

physical properties of these ethylene– $\alpha$ -olefin copolymers.<sup>1,2</sup>

The characterization of SCB with respect to intra- and intermolecular heterogeneity has been of great interest for the last decade. Temperature rising elution fractionation (TREF) and thermal fractionation have proved to be effective ways of characterizing SCB content and distribution.<sup>3–6</sup> TREF produces fractions by the elution of polymer on insert supports in column at successively or stepwise rising temperature. The polymer has been crystallized from dilute solution on insert supports at a very low cooling rate. Such slow crystallization favors macromolecular segregation by SCB content and distribution, with a limited influence of the molecular mass.<sup>3,4</sup> Thermal fractionation is a temperature-dependent segregation process based on recrystallization and reorganization of the ethylene sequence mainly by use of differential scanning calorimetry (DSC).<sup>7</sup> After the particular heat treatment, such as stepwise isothermal segregation technique (SIST),<sup>8</sup> stepwise crystallization (SC),<sup>9</sup> or successive self-nucleation and annealing (SSA),<sup>10</sup> the neighboring ethylene sequences can crystallize independently and subsequently melt at a temperature corresponding to their crystal size or lamellar thickness. Then the final DSC heating run reveals multiple melting points induced by the melting and recrystallization as the re-

Correspondence to: J. Kong (kongmark@mail.china.com).

Contract grant sponsor: Meterage Foundation Project of the National Defense Ministry of China; contract grant number: 61005217.

sult of the heterogeneity of the chain structure of the polymer. There is no actual physical separation of the macromolecules, so intra- and intermolecular heterogeneity are equally assessed. In such thermal fractionations, SSA involves more complex thermal treatments and can be accomplished within a shorter time than that for other thermal fractionations, so it was widely used to characterize the structural heterogeneity of polyolefins or functional polyolefins and miscibility of polyolefin blends.<sup>11–14</sup>

Therefore, it should be possible to combine preparative TREF with SSA to obtain detailed information of the fine structure of LLDPE. In the study reported herein, the 1-butene LLDPE was fractionated by preparative TREF, and subsequently the single-step self-nucleation experiment and SSA thermal fractionation were performed to define the self-nucleation domain and characterize molecular chain heterogeneity of LLDPE and its fractions, respectively. Finally, the statistical terms, including arithmetic mean  $\bar{L}_n$ , weighted mean  $\bar{L}_w$ , and broad index  $\bar{L}_w/\bar{L}_n$ , were introduced to evaluate ethylene sequence length (ESL) and lamellar thickness distribution and molecular chain heterogeneity of LLDPE and its fractions.

## EXPERIMENTAL

### Materials

LLDPE was a commercially available product provided by Qilu Petroleum and Chemical Corp. (Zibo City, Shandong Province, China). The physical parameters of LLDPE used in this study are given in Table I.

### Preparative TREF

Fractionation of the 1-butene LLDPE was accomplished by preparative TREF. The fractionation procedure of TREF involved crystallization of a polymeric dilute solution and a subsequent elution process with solvent in the column. At the crystallization step, the polymer sample was dissolved in xylene at a concentration of 0.006 g/mL in a glass oven, equipped with a temperature controller and stirrer. Glass beads (40–60 mesh), at a concentration of 1.8 g/mL, and 2,2'-methylene-bis(6-*tert*-butyl-4-methyl phenol) (antioxidant 2246), at a concentration of 0.03 mg/mL, were added to the oven, followed by a period of slow cooling from 130 to 25°C, at a rate of 2°C/h, to allow the polymer to crystallize onto the glass beads. Then the glass beads coated with the crystallized sample were filtered and charged to the preparative TREF column (diameter 30 mm, length 300 mm), which was connected to the TREF system. A series of elution temperatures were predetermined at 47, 57, 67, 77, 93, and 105°C. At each temperature, the sample was soaked for 60 min with xylene. Then the elution was performed at a flow rate

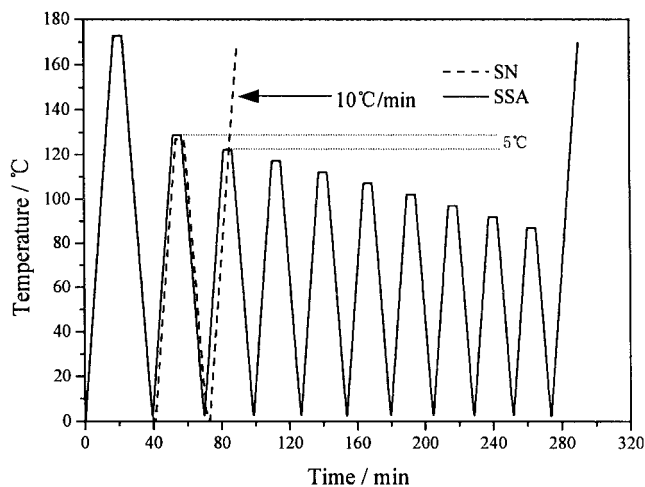


**Figure 1** Schematic representation of single-step self-nucleation and SSA thermal fractionation of LLDPE.

of 5 mL/min until the precipitation did not appear when the elution solution was added to cold acetone. Each fraction was collected and subsequently precipitated by adding excess cold acetone as a nonsolvent. They were finally filtered on a glass filter and dried in vacuum oven for 72 h at 60°C.

### DSC analysis

A modulated differential scanning calorimeter (MDSC2910, TA Instruments, New Castle, DE), equipped with a refrigerated cooling system, was used in this study. The temperature was calibrated with indium (156.6°C) and the heat flow was calibrated with the specific heat of fusion of indium (28.71 J/g) at a scanning rate of 10°C/min. The furnace was purged with dry nitrogen at a flow rate of 50 mL/min. A sample of about 5.0 mg was sealed in an aluminum pan, and the scanning procedure was conducted from –20 to 170°C at a rate of 10°C/min. The sample's crystallinity was calculated by eq. (1), using software supported by TA Instruments,<sup>15</sup> as follows:

$$X_c = \frac{\Delta H_u}{\Delta H_{100}} \times 100\% \quad (1)$$

where  $\Delta H_u$  is the integrated melting enthalpy between 0 and 140°C from the DSC endothermic curve and  $\Delta H_{100}$  is the melting enthalpy of polyethylene crystal with 100% crystallinity, which was set as 287.3 J/g in this study.<sup>16,17</sup>

### Single-step self-nucleation

A schematic representation of the single-step self-nucleation (SN) experiment is shown in Figure 1. The process is described as follows:

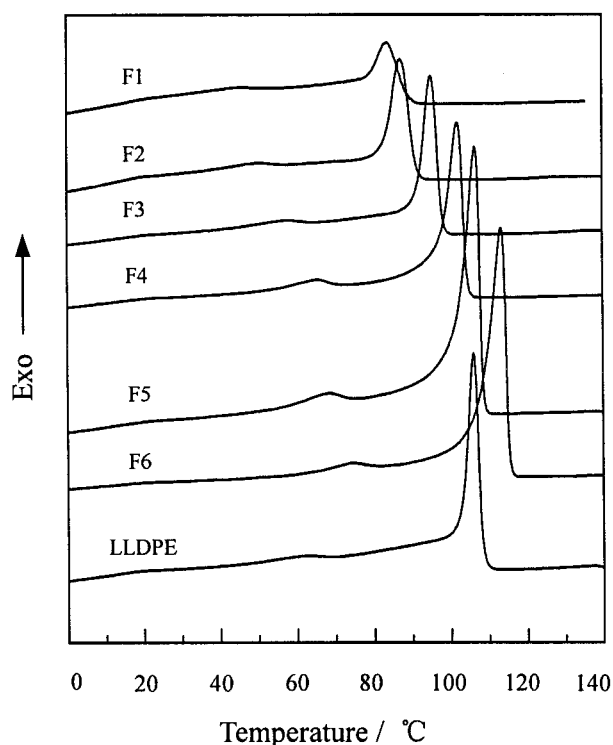


**Figure 2** Crystallization exothermic curves of TREF fractions obtained at different elution temperatures and original LLDPE.

1. The sample was heated to 170°C and maintained at that temperature for 5 min to eliminate the thermal history.
2. The sample was cooled to 0°C to create the so-called initial "standard" state.
3. The sample was heated to a selected thermal treatment temperature ( $T_s$ ) located in the final melting temperature range of initial "standard" state and held at that temperature for 5 min.
4. The sample was cooled to 0°C again, where the effects of thermal treatment would be reflected by the crystallization behavior of the sample.
5. Finally, the sample was heated to 170°C, where the effects of thermal treatment would also be reflected by melting of the sample.

For steps (1)–(5), the DSC scanning rate was 10°C/min.

#### Successive self-nucleation and annealing

A schematic representation of SSA thermal fractionation is also shown in Figure 1. Step (1)–(4) of the single-step self-nucleation experiment were repeated as the first cycle of SSA, and then the following steps were performed as the successive cycles.

5. The sample was heated to a successive predetermined thermal treatment temperature that was 5°C lower than the previous  $T_s$  and held at that temperature for 5 min. Then the sample was cooled to 0°C at the rate of 10°C/min.
6. The sample was heated to 170°C at the rate of 10°C/min, after which the effects of SSA cycles would be reflected.

#### Determination of SCB content

FTIR analysis was performed with a model WQF-310 FTIR spectrometer (Beijing, China). A minimum of 100 scans was used with a resolution of 2  $\text{cm}^{-1}$ . The degree of short-chain branching of polyethylene was determined by using the methyl group absorption band at 1378  $\text{cm}^{-1}$ . Detailed calculation procedures were used according to the literature.<sup>18,19</sup>

## RESULTS AND DISCUSSION

#### Temperature rising elution fractionation

Polyethylene fractions were prepared corresponding to the predetermined elution temperature. The DSC exothermic curves and endothermic curves for fractions and the original LLDPE are presented in Figure 2 and Figure 3, respectively. The crystallinity, content of SCB, and melting temperature of fractions plotted against the corresponding elution temperature are shown in Figure 4 and Figure 5, respectively.

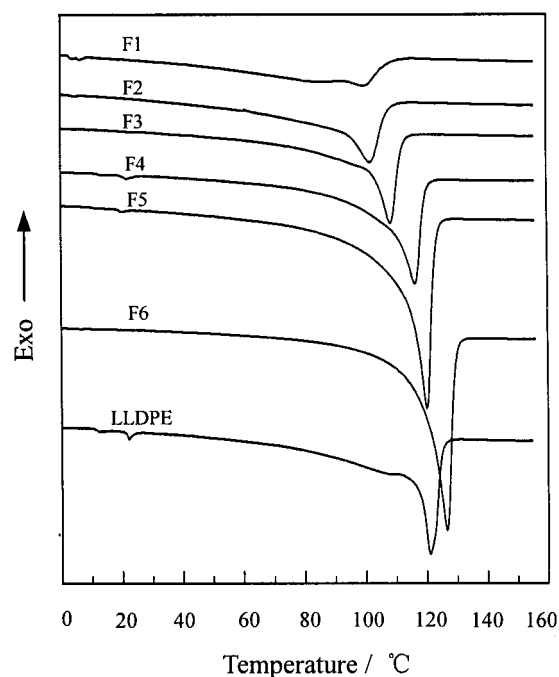


**Figure 3** Melting endothermic curves of *p*-TREF fractions obtained at different elution temperatures and original LLDPE.

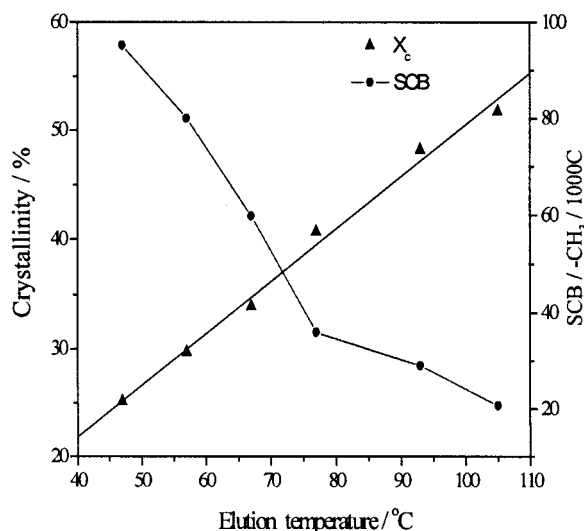


**Figure 4** Dependency of crystallinity and SCB of fractions on elution temperature.

Evidently, the increasing crystallinity, melting temperature, and decreasing content of SCB are obtained with the increase in elution temperature. In particular, the linear relationship can be verified from the plots of crystallinity and melting temperature against elution temperature. These results are in accordance with those of Hosoda and Mirebella.<sup>20,21</sup> In this article, LLDPE is a copolymer of ethylene and 1-butene, and the content and distribution of SCB are the key factors to its melting temperature and crystallizability. Thus the content of SCB plays an important role in the crystallization behaviors from dilute solution and subsequent elution of polymer according to the elution thermodynamic mode of TREF.<sup>22</sup> This further proves that TREF separates LLDPE according to the crystallizability or the content of SCB. As can be seen from Figure 3, the endothermic curve for the original LLDPE involves a higher-temperature melting peak and a broad lower-temperature melting peak, whereas the endothermic curves for all the fractions exhibit only a single melting peak with a long tail toward low temperature. This suggests that fractions have less heterogeneity than that of the original LLDPE. In addition, it should be pointed out that the endothermic curve for the first fraction (F1) presents two low-temperature melting peaks that are the same as those of the original LLDPE, which may be attributed to its broad low elution temperature range.

### Single-step self-nucleation

As described above, the DSC endothermic curves for fractions have a single melting peak with a long tail toward low temperature, although fractions have less heterogeneity than that of the original LLDPE. A more

specialized heat treatment such as SSA thermal fractionation, which is able to assess both intra- and intermolecular heterogeneity, must be accomplished to quantitatively characterize the heterogeneities of fractions. During this process, described in the experimental section, the first self-nucleation temperature ( $T_s$ ) is more important than the intervals of  $T_s$ , isothermal self-nucleation, or annealing time and scanning rate.<sup>23</sup> The first  $T_s$  should be high enough to melt most of the polymer, but low enough to leave some crystal fragments that can act as nuclei.<sup>24</sup> Thus, in this section, the first  $T_s$  of LLDPE is to be determined in a single-step self-nucleation analysis.

Figures 6 and 7 show, respectively, DSC exothermic and endothermic curves for LLDPE after thermal treatments at different  $T_s$  values. The detailed parameters of DSC measurements are listed in Table II.

It is obvious that all the exothermic peaks and endothermic peaks shift to higher temperature with decreasing  $T_s$  values. Because all  $T_s$  values are higher than the melting temperature of the standard state ( $T_{m1} = 121.3^\circ\text{C}$ , as described in Table II), polyethylene is in the melting or partial melting region, where there exists some unmelted crystal fragments that could act as nucleus during the cooling process. With the effects of self-nucleation, polyethylene can crystallize with narrower supercooling and melt on higher temperature. The effects of  $T_s$  on crystallization temperature  $T_m$  and crystallinity of LLDPE are presented in Figures 8 and 9, respectively.

As is shown in Figure 8, if the value of  $T_s$  is higher than  $126^\circ\text{C}$ , the onset crystallization temperature and peak crystallization temperature show no marked difference with the increase in  $T_s$ . The reason is that the nucleus density remained constant and minimal in the

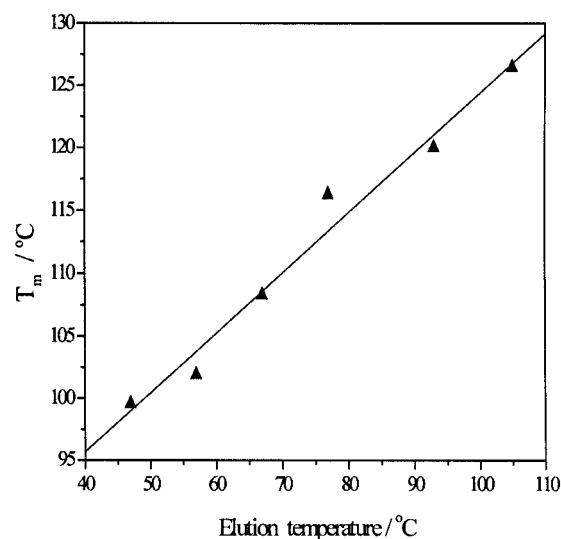


**Figure 5** Dependency of melting temperature of fractions on elution temperature.

TABLE I  
Physical Parameters of Commercial LLDPE

Designation	Comonomer	Density <sup>a</sup> (g/cm <sup>3</sup> )	MI <sup>a</sup> (g/10 min)	$\bar{M}_w^b$ (g/mol)	$\frac{\bar{M}_w}{\bar{M}_n}^b$	$X_c^c$
DFDA 7042	1-Butene	0.90	2.0	91,339	3.28	38%

<sup>a</sup> The data were taken from chemical data sheets published by the manufacturer.

<sup>b</sup> The molecular weight and molecular weight distribution were measured by using a PL220 high-temperature size-exclusion chromatography (PL220, Shropshire, UK). 1,2,4-Trichlorobenzene was used as the elution solvent with a flow rate of 1.0 mL/min. The operating temperature was 160°C. Polystyrene standards were used for making the calibration curve.

<sup>c</sup> Crystallinity was determined by use of a wide-angle X-ray diffractometer (Philips, The Netherlands) at ambient temperature. The instrument was equipped with a graphite homochromatic instrument, Cu anticathode, 40 kV, 40 mA, scanning rate 2.5°/min,  $2\theta = 5\text{--}50^\circ$ . Crystallinity of LLDPE was calculated by a computer peak-dividing program.

melting region. If  $T_s$  is in the region of 123 and 126°C, the onset crystallization temperature and peak crystallization temperature increase dramatically with decreasing  $T_s$ . The reason is that  $T_s$  was high enough to melt most of the polymer, but low enough to allow the survival of some crystal fragments. Thus the small reduction of  $T_s$  resulted in the increases in nucleation density, crystallization temperature, and melting temperature. If the value of  $T_s$  is lower than 123°C, two endothermic peaks can be seen in Figure 7, which means annealing has occurred. It should be noticed that no onset crystallization temperature is observed at 123°C (Fig. 6). It is suspected that crystallization starts almost immediately upon cooling, leaving no obvious trace of a perfectly flat baseline before the onset of crystallization attributed to the high concentration of nucleus.

On the other hand, as can be seen from Figure 9, the melting temperature and crystallinity increase with the decrease in  $T_s$  after self-nucleation or annealing. When the value of  $T_s$  is higher than 126°C,  $T_m$  and crystallinity both remain constant. However, when the  $T_s$  value is lower than 126°C, self-nucleation or annealing ( $T_s = 123^\circ\text{C}$ ) occurs. Because of the effects of self-nucleation or annealing, polyethylene is thus formed from perfect and thicker lamellae and has higher crystallinity and  $T_m$ . The so-called domain of self-nucleation of an isotactic polypropylene (i-PP) was extensively investigated by Fillon.<sup>25,26</sup> In this article, similar domains of LLDPE by single-step self-nucleation analysis are shown in Figure 10. (1) In domain I,  $T_s$  is higher than 126°C. Both crystallization and melting behaviors of polyethylene are similar to those of the standard state. (2) In domain II,  $T_s$  is in the

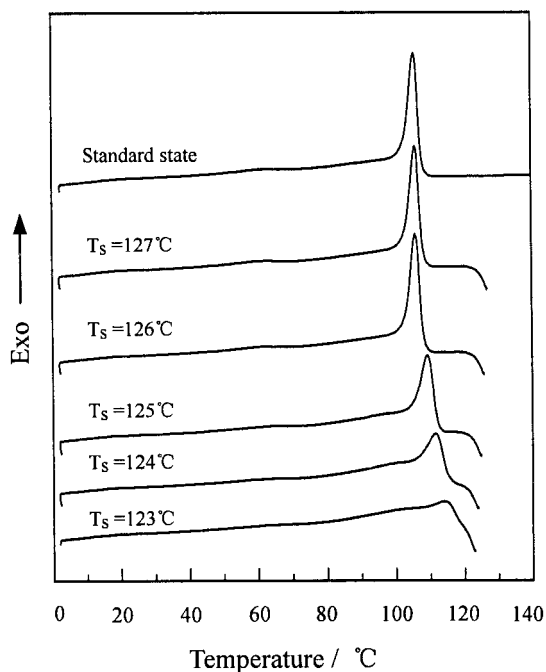


Figure 6 Crystallization exothermic curves of LLDPE treated at different  $T_s$  and standard state.

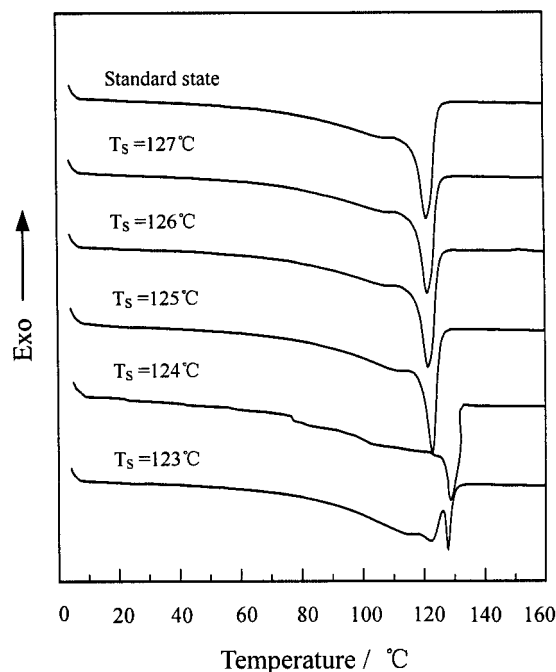


Figure 7 Melting endothermic curves of LLDPE treated at different  $T_s$  and standard state.

TABLE II  
Detailed Information of Single-Step Self-Nucleation Experiment<sup>a</sup>

$T_s$ (°C)	$T_c$ (°C)		$\Delta H_c$ (J/g)	$T_m$ (°C)		$X_c$ (%)
	$T_{onset}$	$T_{peak}$		$T_{m1}$	$T_{m2}$	
St	111.3	105.8	115.1	121.3	—	35.8
123	—	114.1	—	127.8	122.3	36.1
124	119.2	111.6	119.3	123.3	—	37.1
125	115.0	109.3	110.6	122.6	—	36.9
126	111.4	106.0	109.3	121.3	—	35.6
127	111.5	105.9	110.0	121.4	—	35.8

<sup>a</sup>  $T_s$ , self-nucleation or annealing temperature;  $T_{onset}$ , onset temperature of the primary peak on DSC exotherm;  $T_{peak}$ , peak temperature of the primary peak on DSC exotherm;  $\Delta H_c$ , enthalpy of crystallization;  $T_{m1}$ , peak temperature of the primary peak on DSC endotherm;  $T_{m2}$ , peak temperature of low temperature peak on DSC endotherm;  $X_c$ , the melting enthalpy was integrated between 10 and 140°C.

region of 123 and 126°C and high enough to melt most of the polyethylene, but low enough to allow the survival of some crystal fragments as nuclei for crystallization. (3) In domain III,  $T_s$  is lower than 123°C and the extra peak appears and annealing occurs.

### Successive self-nucleation and annealing

The self-nucleation domain of LLDPE has been described in the single-step self-nucleation experiment. In the current SSA process, the first  $T_s$  is to be predetermined in domain II of the original LLDPE. The processes of predetermination of the first  $T_s$  value of TREF fractions of LLDPE are similar to that of the original LLDPE, described earlier in the section on single-step self-nucleation. Thus, after SSA heat cycles, the plots of final heating endothermic curves of TREF fractions and the original LLDPE are all shown in Figure 11.

Obviously, the final heating runs of fractions and the original LLDPE present multiple endothermic peaks corresponding to the number of SSA cycles. Each endothermic peak can represent the melting of crystals formed from molecules having very similar ESL, so it is suspected that the multiple endothermic peaks can be mainly attributed to the lamellar thickness or ESL heterogeneity.<sup>27</sup> The plots in Figure 11 clearly indicate the heterogeneity existing inside either original LLDPE or fractions. Because each endothermic peak is proportional to the amount of crystals with the same stability, the differential normalized area under such fusion is proportional to the amount of lamellae that melt in the temperature interval. The lamellar thickness and ESL are related to the melting temperature, so the lamellar thickness of polyethylene can be determined by using the Thomson–Gibbs equation [eq. (2)]<sup>28</sup>:

$$L_c = 2\sigma_e T_m^0 / \Delta H_u (T_m^0 - T_m) \quad (2)$$

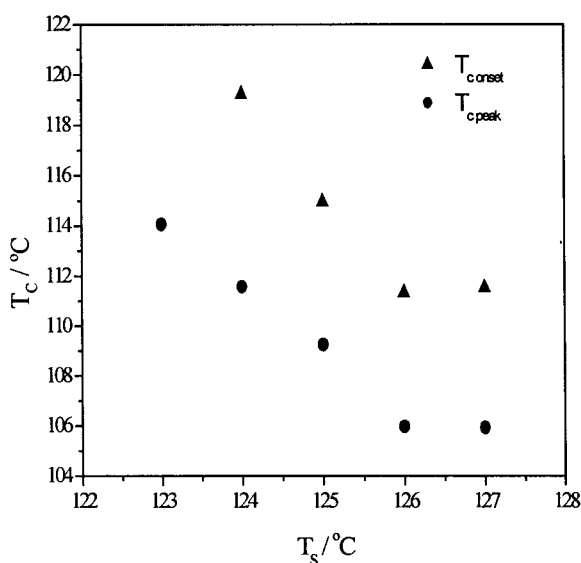


Figure 8 Dependency of onset and peak temperature of crystallization of LLDPE on  $T_s$ .

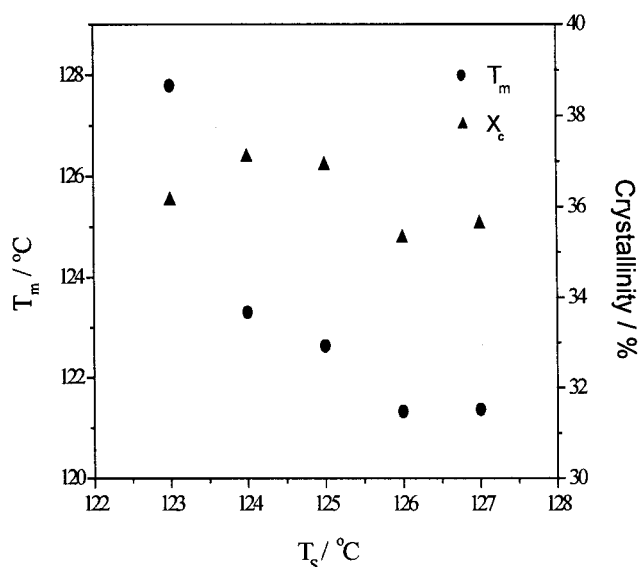
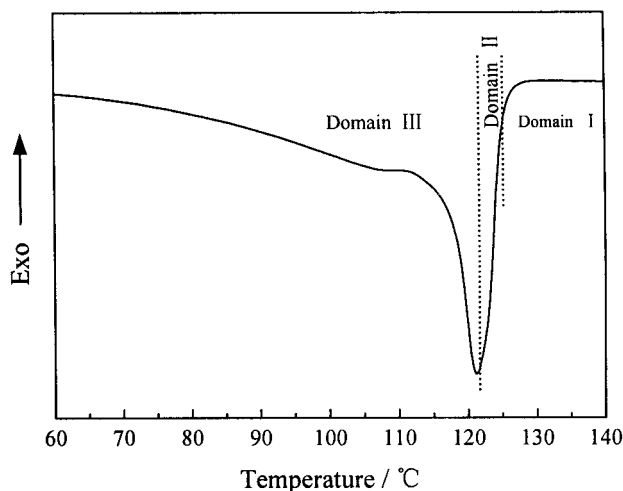


Figure 9 Dependency of melting temperature and crystallinity of LLDPE on  $T_s$ .



**Figure 10** Melting endotherm of LLDPE in the "standard" state, Domains I, II, and III refer to complete melting, self-nucleation, and annealing region, respectively.

where  $L_c$  is lamellar thickness,  $T_m$  is the observed melting point,  $T_m^o$  is the equilibrium melting point of an infinitely thick polyethylene crystal (414.5 K),  $\sigma_e$  is the surface energy of polyethylene crystal ( $70 \times 10^{-3}$  J/m<sup>2</sup>), and  $\Delta H_u$  is the enthalpy of fusion per unit volume ( $288 \times 10^6$  J/m<sup>3</sup>).<sup>29</sup> The average ethylene sequence length (ASL) can be calculated by the following equation<sup>30</sup>:

$$\text{ASL} = 0.2534X/(1 - X) \quad (3)$$

where  $X$  represents the CH<sub>2</sub> mole fraction of polyethylene, which is well correlated to the melting temperature, using the Keating method,<sup>31</sup> by the following equation:

$$-\ln(\text{CH}_2 \text{ mole fraction}) = -0.331 + 135.5/T_m \text{ (K)} \quad (4)$$

It should be pointed out the crystallization of a short-chain branching polyethylene may differ from that of linear paraffin used as a model in the Keating method. However, the use of linear paraffin as a reference<sup>32</sup> appears to provide results in some cases, in the absence of better standard samples. By use of eqs. (2)–(4), the proportion being melted as a function with the lamellar thickness and ESL of TREF fractions can be determined. As the representation, the derived lamellar thickness distribution for three different fractions, including F1, F2, and F3, are presented in Figures 12 and 13, respectively.

As can be seen from Figures 12 and 13, the distributions of lamellar thickness and ethylene sequence length are similar to the results of SSA thermal fractionation curve described in Figure 11, which indicates

that the higher elution temperature fraction (F5) had a broader lamellar thickness of 2–16 nm, and ESL distribution of 3–49 nm, respectively. This suggests that F5 has a more heterogeneous molecular structure than that of the lower elution temperature fractions (F1 and F3). To investigate the heterogeneity of ethylene-1-olefin copolymers quantitatively, Keating introduced statistical terms to describe the polydispersity of ethylene sequence length.<sup>33</sup> Both the ethylene sequence length and lamellar thickness distributions of narrow molecular distribution metallocene-catalyzed ethylene- $\alpha$ -olefin copolymers, after SIST thermal fractionation, were previously discussed by Zhang.<sup>29</sup> Herein, the statistical terms, arithmetic mean  $\bar{L}_n$ , weighted mean  $\bar{L}_w$ , and the broadness index  $I$ , are also introduced and shown as follows:

$$\bar{L}_n = \frac{S_1L_1 + S_2L_2 + \dots + S_iL_i}{S_1 + S_2 + \dots + S_i} = \sum f_i L_i \quad (5)$$

$$\bar{L}_w = \frac{S_1L_1^2 + S_2L_2^2 + \dots + S_iL_i^2}{S_1L_1 + S_2L_2 + \dots + S_iL_i} = \frac{\sum f_i L_i^2}{\sum f_i L_i} \quad (6)$$

$$I = \bar{L}_w / \bar{L}_n \quad (7)$$

where  $S_i$  is the normalized peak area and  $L_i$  is the ESL or lamellar thickness. After deriving the melting tem-

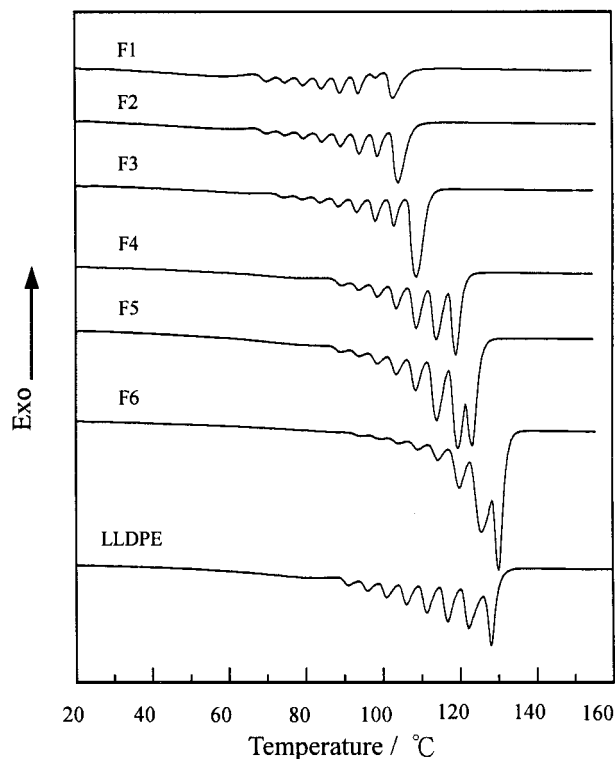


**Figure 11** SSA thermal fractionation curve of LLDPE and fractions obtained at different elution temperatures.

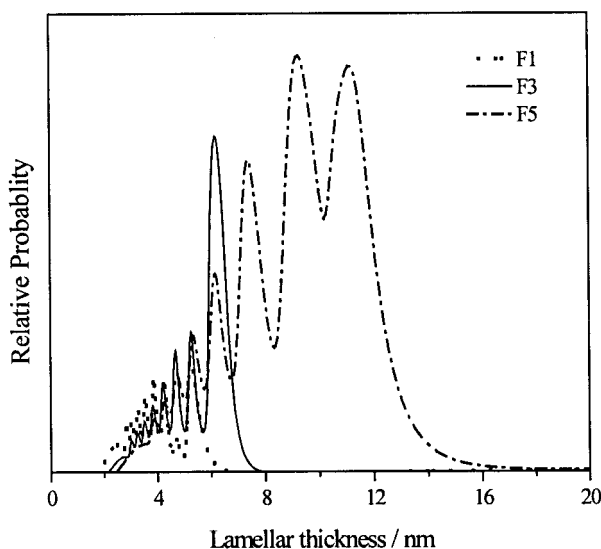


Figure 12 Derived lamellar thickness distribution for fractions by using SSA and the Thomson–Gibbs equation.

perature and normalized peak area of multiple endothermic peaks (as described in Fig. 11), with the Thomson–Gibbs equation and the Keating method, three terms of ethylene sequence length and lamellar thickness for all the fractions and original LLDPE are given in Table III. It can be seen from Table III that the broadness index of fraction is less than that of the origin LLDPE, which suggests that TREF fractions have less heterogeneity of either ESL or lamellar thickness than that of the origin LLDPE. Because the intra- and intermolecular heterogeneities of polyethylene are equally assessed in SSA thermal fractionation, the fractions have less intra- and intermolecular heterogeneities than that of the original LLDPE.

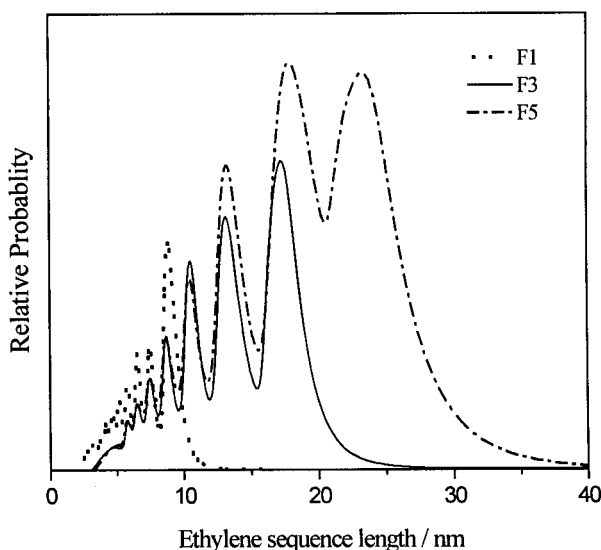


Figure 13 Derived ethylene sequence length distribution for fractions by using SSA and the Keating method.

TABLE III  
Ethylene Sequence Length and Lamellae Thickness Distributions of Polyethylene

Fraction	Ethylene sequence length distribution			Lamellar thickness distribution		
	$\bar{L}_n$ (nm)	$\bar{L}_w$ (nm)	<i>I</i>	$\bar{L}_n$ (nm)	$\bar{L}_w$ (nm)	<i>I</i>
F1	6.1	6.5	1.07	4.1	4.2	1.04
F2	6.8	7.3	1.07	4.5	4.6	1.04
F3	8.3	8.9	1.07	5.2	5.4	1.04
F4	12.0	13.1	1.09	6.8	7.2	1.06
F5	15.3	17.4	1.14	8.1	8.6	1.08
F6	26.0	35.0	1.31	12.4	13.9	1.11
LLDPE	18.7	24.6	1.32	9.1	10.6	1.16

## CONCLUSION

In conclusion, the cross-fractionation of preparative TREF and SSA is an effective method of characterizing the fine structure of LLDPE. The TREF analysis indicates that polyethylene fractions have less intermolecular heterogeneity than that of the original LLDPE. In the single-step self-nucleation analysis, Domain II of LLDPE was determined in the region of 123–126°C. In this region, the self-nucleation temperature of SSA is high enough to melt most of the polyethylene, but low enough to allow the survival of some crystal fragments to act as nuclei in crystallization. By SSA thermal fractionation, the multiple melting peaks of either original LLDPE or fractions are presented corresponding to the number of SSA cycles. The broadness index of either ESL or lamellar thickness of TREF fractions is smaller than that of the original LLDPE, which further indicates that TREF fractions have less inter- and intraheterogeneity of both ESL and lamellar thickness than that of the original LLDPE.

This study was financially supported by a Meterage Foundation Project (contract grant number: 61005217), from the National Defense Ministry of China.

## References

1. Fu, Q.; Chiu, F. C.; He, T. B.; Liu, J. P.; Hsieh, E. T. *Macromol Chem Phys* 2001, 202, 927.
2. Zhang, M.; Lynch, D. T.; Wanke, S. E. *Polymer* 2001, 42, 3067.
3. Wild, L.; Ryle, T. R.; Knobloch, D. C.; Peat, I. R. *J Polym Sci Polym Phys Ed* 1982, 20, 441.
4. Deffoor, F.; Groeninckx, G.; Schouterden, P.; Van Der Heijden, B. *Polymer* 1992, 33, 3878.
5. Soares, J. S. P.; Hamielec, A. E. *Polymer* 1995, 36, 1639.
6. Starck, P.; Rajanen, K.; Löfgren, B. *Thermochimica Acta* 2002, 395, 169.
7. Adisson, E.; Ribeiro, M.; Deffieux, A.; Fontanille, M. *Polymer* 1992, 33, 4337.
8. Kamiya, T.; Ishikawa, T.; Kambe, S.; Ikegami, N.; Nishibu, N.; Hattori, T. *Proc SPE Tech Papers, ANTEC*, 90, 871.
9. Drummond, K. M.; Hopewell, J. L.; Shanks, R. A. *J Appl Polym Sci* 2000, 78, 1009.



10. Müller, A. J.; Hernandez, Z. H.; Arnal, M. L.; Sanchez, J. J. *J Polym Bull* 1997, 39, 465.
11. De Gascue, B. R.; Mendez, B.; Manosalva, J. L.; Lopez, L.; Quiteria, V. R. S.; Müller, A. J. *Polymer* 2002, 43, 2151.
12. Marquez, L.; Rivero, I.; Müller, A. J. *Macromol Chem Phys* 1999, 200, 330.
13. Czaja, K.; Sacher, B.; Bialek, M. *J Therm Anal Calorim* 2002, 67, 547.
14. Arnal, M. L.; Sanchez, J. J.; Müller, A. J. *Polymer* 2002, 42, 6877.
15. Blundell, D. J.; Beckett, D. K.; Wilcocks, P. H. *Polymer* 1981, 22, 704.
16. Kong, J.; Fan, X.-D.; Jia, M. *J Appl Polym Sci* 2004, 93, 2542.
17. Wunderlich, B.; Cormier, C. M. *J Polym Sci Part A-2* 1967, 5, 987.
18. Neves, C. J.; Monteiro, E.; Habert, A. C. *J Appl Polym Sci* 1993, 50, 817.
19. Lei, W.-Y.; Gu, F.; Zhang, W. *Polymer Physics Experiment*; Northwestern Polytechnical University Press: China, 1994.
20. Hosoda, S. *Polym J* 1988, 20, 383.
21. Mirabella, F. M. *J Polym Sci Part B: Polym Phys* 2001, 39, 2819.
22. Borrajo, J.; Cordon, C.; Garella, J. M.; Toso, S.; Goizueta, G. *J Polym Sci Part B: Polym Phys* 1995, 33, 1627.
23. Arnal, M. L.; Balsamo, V.; Ronca, G.; Sanchez, A.; Müller, A. J.; Canizales, E.; de Navarro, C. U. *J Therm Anal Calorim* 2000, 59, 451.
24. Balsamo, V.; Paolini, Y.; Ronca, G.; Müller, A. J. *Macromol Chem Phys* 2000, 201, 2711.
25. Fillon, B.; Lotz, B.; Thierry, A.; Wittmann, J. C. *J Polym Sci Part B: Polym Phys* 1993, 31, 1395.
26. Fillon, B.; Thierry, A.; Wittmann, J. C.; Lotz, B. *J Polym Sci Part B: Polym Phys* 1993, 31, 1407.
27. Ungar, G.; Kellar, A. *Polymer* 1987, 28, 1899.
28. Darras, O.; Seguela, R. *Polymer* 1993, 34, 2946.
29. Starck, P. *Polym Int* 1996, 40, 111.
30. Zhang, F. J.; Liu, J. P.; Fu, Q.; Huang, H. Y.; Hu, Z. H. J.; Yao, S. H.; Cai, X. Y.; He, T. B. *J Polym Sci Part B: Polym Phys* 2002, 40, 813.
31. Keating, M.; Lee, I. H.; Wong, C. S. *Thermochim Acta* 1996, 284, 47.
32. Kapoglanlan, S. A.; Harrison, I. R. *Thermochim Acta* 1996, 288, 239.
33. Keating, M.; McCord, E. E. *Thermochim Acta* 1994, 243, 129.